

## MASS FLUX MEASUREMENT OF TWO-PHASE SPRAY BY AN IMPULSE PROBE AND PDPA

M.A. Rahman<sup>1\*</sup>, F. Vakili<sup>2</sup>, M.A. Islam<sup>3</sup>, B.A. Fleck<sup>4</sup>, D. Matovic<sup>5</sup> and S. Sanders<sup>1</sup>

<sup>1</sup> Department of Chemical and Materials Engineering, University of Alberta, Canada

<sup>2</sup> Department of Mechanical Engg., Ecole Polytechnique Fédérale de Lausanne, Switzerland

<sup>3</sup> Bangladesh University of Engineering and Technology, Bangladesh

<sup>4</sup> Department of Mechanical Engineering, University of Alberta, Canada

<sup>5</sup> Department of Mechanical and Materials Engineering, Queen's University, Canada

### ABSTRACT

Mass flux measurement of droplets in multiphase atomization is a challenging task. Advanced laser diagnostics such as the Phase Doppler Particle Anemometer (PDPA) are not capable of accurately measuring the droplet mass flux in a dense spray due to the higher rejection of non-spherical droplets by the PDPA. A combined measurement of momentum data from the impulse sensor (IS) and velocity data from the PDPA provides a reasonable estimate of mass flux data in the two phase spray envelope. The mass flux data obtained by the coupled PDPA+IS will facilitate the estimation of the void fraction in multiphase dense spray which will be very beneficial to the design of industrial multiphase nozzles.

**Keywords:** Two Phase, Atomization, Droplet, Mass Flux, Impulse Probe, PDPA.

### 1. INTRODUCTION

Gas-assisted as effervescent atomization is a popular technique in industrial applications since the process can generate more dispersed and smaller droplets because of the greater aerodynamic shear stress on the liquid phase. However, two-phase gas/liquid atomization characterization is a challenging task [1-4]. It is very common to have pulsations in gas-assisted atomization. Our experimental observations indicate that available experimental techniques, such as Phase Doppler Particle Anemometer (PDPA), are not able to characterize fully the multiphase spray. The PDPA technique can only reliably measure the droplet velocity. However, PDPA cannot measure the mass flux very accurately due to the higher rejection rate of non-spherical droplets. Thus, using the velocity data from the PDPA and force data from the Impulse Sensor (IS) can assist in reliably calculating the mass flux.

A study in fuel spray indicated that spray momentum flux information is critical to characterize a spray since momentum information determines the spray penetration, spray cone, air entrainment and mixing potential in the reactor (jet bed interaction). In the experiment, they used an impingement force measurement technique and validated the results using the macroscopic spray visualization method [5]. Several other studies can be found in the literature describing the use of spray momentum flux to study the spray characteristics [6, 7]. A simulation of water jet which was validated by the

experimental data indicated that the peak of an impulsive impact force in the pulsating spray was found to be 3 times greater than that of the continuous water jet [8]. In another study, the impact probe was used to measure the spray momentum in multiphase spray [9]. Also, a piezoelectric dynamometer was used to measure high-speed water jet characteristics [10].

In this study, two phase gas/liquid spray momentum flux and mass flux were measured using a coupled PDPA+IS technique. The force data obtained from an impulse probe is coupled with the precise velocity data obtained from the PDPA technique to estimate the mass flux in a dense spray. This novel method will assist in understanding the fundamental behavior of multiphase spray in industrial applications. This study will also help to answer some of the fundamental questions about the mass flux distribution in the two phase dense spray. This will aid in the improvement of the multiphase atomization design process in industrial applications.

### 2. THEORY

Consider a steady flow impinging on a perpendicular flat plate as shown in Figure 1. The streamline in Figure 1 divides into two segments. The streamline above the dividing line flows over the plate and the stream line going under the dividing line flows under the plate. Since the flow of the dividing stream lines cannot pass through the plate, the fluid must come to rest at a point. Thus,

fluid along this line slows down without deflecting the plate and it stagnates. The Bernoulli's equation along the stagnation streamline gives:

$$P_u + \frac{1}{2} \rho u_u^2 = P_s + \frac{1}{2} \rho u_s^2 \quad (1)$$

here, the subscript 'u' indicates the upstream condition, subscript 's' indicates the stagnation condition and  $\rho$  indicates the density of the fluid.

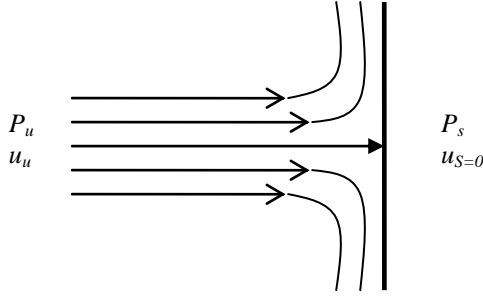


Fig 1. Stagnation point flow. Here,  $P_u$  is the upstream pressure,  $u_u$  is the upstream velocity,  $P_s$  is the stagnation pressure,  $u_s$  is the stagnation velocity.

Since at the stagnation condition the stagnation velocity is zero, the Equation (1) can be written as follows:

$$P_u + \frac{1}{2} \rho u_u^2 = P_s \quad (2)$$

The stagnation pressure is the highest pressure in the flow. The effects of the gas phase pressure are negligible as the density of air is considerably less than the density of water. The piezoelectric sensors only measure the dynamic pressure of the fluid motion, which reflects the momentum flux of droplets impacting on the tip of sensor. In any axial location perpendicular to the spray, the liquid mass flux is conservative. Thus, the liquid mass flux exiting the nozzle orifice should be equal to the integral mass flux at any cross section in the spray. One can write:

$$m_T = \sum_{i=1}^N m_x \quad (3)$$

where, 'x' indicates the axial location, 'i' indicates local mass flux, 'T' indicates total,  $N$  is the total number of droplets and  $m_x$  is the mass flux in the axial direction, with the units of  $\text{kg/s.m}^2$  or  $(\text{m}^3/\text{s.m}^2)$ . The mean dynamic force was measured inside the spray envelope at a particular point at different radial positions ( $r = 0$  to  $80$  mm) and axial distances (such as  $15D$ ,  $30D$ ,  $60D$ ,  $120D$ ) of the spray. Since this force is the combined effect of water mass flow rate and velocity of droplets at this point, the water mass flow rate can be obtained if the mean droplet velocity is known at this point. The mean droplet velocity can be obtained using the PDPA at those specific points.

### 3. EXPERIMENTAL SETUP

In this study, a one-quarter scale version of a patented nozzle [11] was used in the set-up shown in Figure 2. The full scale nozzle is used in a fluidized bed coker for heavy oil upgrading. In the laboratory experiment, a feeding conduit of  $36.8$  cm length and  $6.35$  mm ID was used prior to the nozzle. The nozzle diameter ( $D$ ) was  $3.10$  mm. This nozzle assembly was mounted on a 3-D automated traversing rig. The experiments were performed using mixtures of water ( $0.04$  L/s to  $0.11$  L/s) with air ( $0.16$  L/s to  $0.48$  L/s), which gave air to liquid mass ratios ( $\beta$ ) of  $1$  to  $4\%$ . Mean drop size was measured using a 2-D Phase Doppler Particle Anemometer (PDPA) [12]. The working principle of the PDPA can be found in the literature [13-17]. The force generated from droplets in any axial cross section of the spray was measured by a piezoelectric force sensor, Kistler 9203, and a charge amplifier, Kistler 5010B. This force sensor is extremely sensitive and capable of resolving the contact force from few mN to  $100$  N. A charge amplifier was used to convert the transmitted charge from a high impedance piezoelectric force into a high level output voltage and provide excitation power en route. This high level voltage output can be read online using an oscilloscope. In the current experiment, a digitizing oscilloscope Tektronix TDS 410A with record length of  $15000$  points per minute was used to read the output voltage.

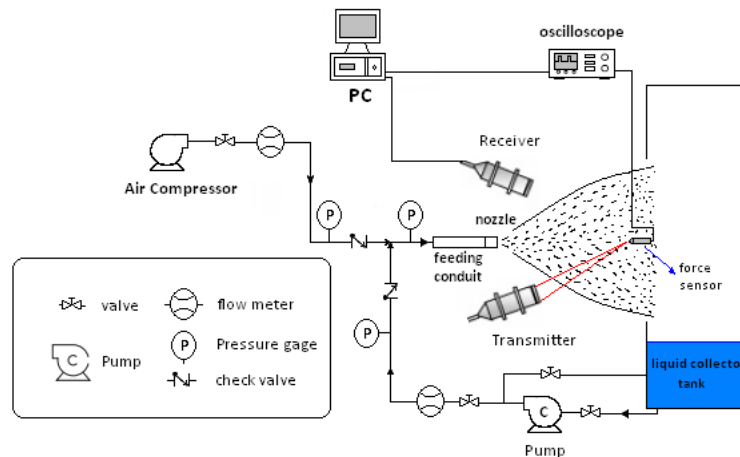


Fig 2. Experimental set-up.

A quartz force sensor as shown in Figure 3(a) measured the average dynamic force, which was generated by the impingement of droplets in the IS. The device can measure the force in the range of a few N up to 400 kN. The quartz force sensor is mounted tightly in a welded steel mounting device. To minimize the deflection of surrounding droplets on the measurement point, a mounting device of aerodynamic shape was used. The quartz force sensor yields an electric charge proportional to the mechanical load applied at the tip of the sensor. Figure 3(b) shows the schematic of the charge amplifier used to convert the transmitted charge into a high level output voltage.

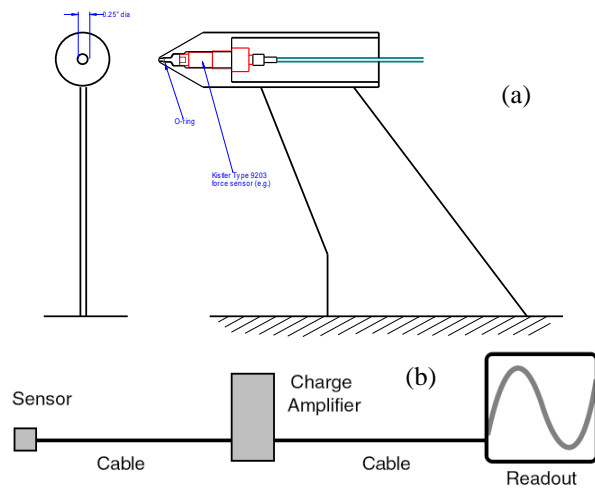


Fig 3. (a) Quartz force sensor and (b) the charge amplifier output

#### 4. RESULTS AND DISCUSSIONS

Spray patterns indicating poor atomization and well atomization are depicted in Figure 4. Due to greater pulsations in the flow associated with poor atomization in Figure 4 (a), the droplets are non-uniform. However, due to less pulsation for the good spray of Figure 4 (b), the droplets are nicely dispersed and uniform in the spray envelope, giving the pattern shown in the figure.

In Figure 5, droplet force data obtained by the IS method and droplet mass flux data obtained by the PDPA are depicted. Data were collected at 2% air to liquid mass ratio ( $\beta$ ), 60D nozzle downstream and 482 kPa mixing pressure. Data obtained from the PDPA is not symmetrical in both the radial directions due to the reduced visibility for the receiver if one traverses from one direction to another direction. Whereas the force data is uniform in both radial directions since there is no issues of optical visibility with the IS measurement.

In Figure 6, the effect of the air to liquid mass ratio on the droplet force is presented. The data were collected at 60D nozzle downstream from the tip of the nozzle. Here, D corresponds to the nozzle diameter of 3.10 mm. It is notable that if the air to liquid mass ratio increases, the force produced by the droplets also increases. At higher air to liquid mass ratios, the air phase momentum is transferred to the liquid phase and provides greater force

in the droplets. If the droplet travels to the downstream of the spray, the droplet loses its momentum, providing less force further downstream. However, in the case of 1% air to liquid mass ratio, the intermittent pulsation in the spray still provides slightly higher momentum, which is transferred farther downstream of the nozzle. Thus, 1% air to liquid mass ratio in Figure 6 still shows marginally higher force values after  $r = 30$  mm downstream.

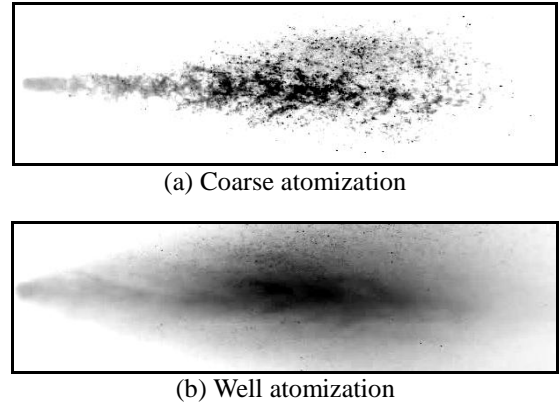


Fig 4. Spray images.

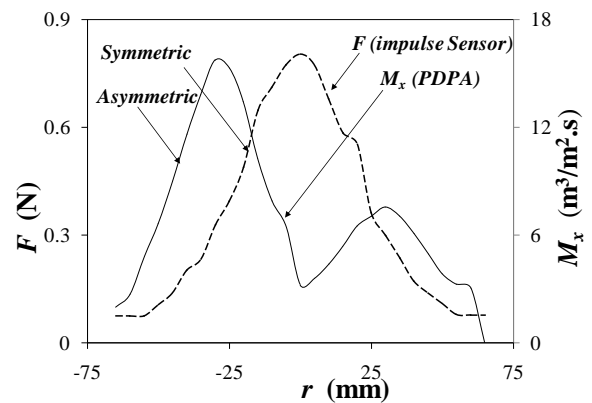


Fig 5. Comparison between the PDPA and IS technique.

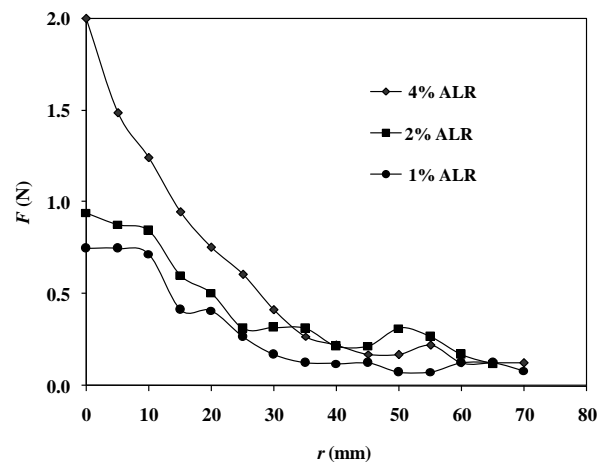


Fig 6. Variation of Force ( $F$ ) produced from a spray with air to liquid mass ratio ( $\beta$ ) and radial distances ( $r$ ) at 60D nozzle downstream.

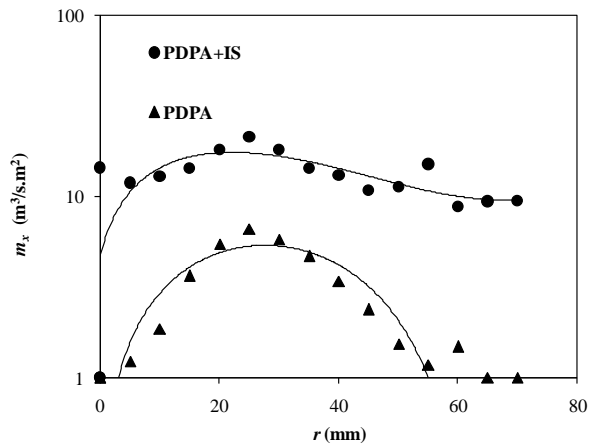


Fig 7. Mass flux ( $m_x$ ) produced from a spray with changing radial distances ( $r$ ) at 60D nozzle downstream. The mixing pressure was 482 kPa and air to liquid mass ratio was 2%.

The mass flux distribution ( $m_x$ ) with changing radial positions is depicted in Figure 7. It is notable that the  $m_x$  estimation by the PDPA alone is much less than the  $m_x$  estimation by the coupled PDPA+IS method. The PDPA method provides a very reliable measurement of mass flux when the spray is optically transparent (not a dense spray) and spherical dispersed droplets are present in the spray envelope. In a dense spray where many non-spherical droplets are present, the PDPA rejects the non-spherical droplet when it estimates the mass flux. Thus, the PDPA always underestimates the mass flux values for a dense spray which contains non-spherical droplets. In Figure 8 the void fraction profile at 60D nozzle downstream obtained by the PDPA and PDPA+IS method is presented. From Figure 8 it is also confirmed that the void fraction estimation by the PDPA alone in a particular cross section perpendicular to the spray axial direction is higher since the PDPA rejects the non-spherical droplets. Improved void fraction estimation is observed for the PDPA+IS method.

The integrated mass flux was calculated in a particular plane at positions of 15D, 30D, 60D and 120D downstream of the discharge. Figure 9 shows the integrated mass flux ( $m_x$ ) values at increasing axial lengths ( $L$ ). Figure 9 also shows how the liquid phase mass is conserved at any section of a spray. In Figure 9, the actual mass flux values were obtained from the known input liquid content in our experiment. It is evident that the mass flux obtained by the PDPA+IS method better conserves the input liquid content compared to the strict PDPA method.

Figure 10 shows the integrated void fraction ( $\alpha$ ) values at increasing axial direction of the spray ( $L$ ). The void fraction estimation by the PDPA alone is greater than calculations based on the PDPA+IS method. Moreover, with increasing axial distances the  $\alpha$  increases since the cone shape of the spray provides a greater area for the same amount of input liquid in a space. However, the  $\alpha$  values shows slightly higher at 15D nozzle downstream. At 15D the liquid ejected from a nozzle tip does not break-up fully into droplets. Once the droplets

finish breaking-up at a position near 30D, the void spaces at that section go down since the tiny droplets occupy most of the area in the spray envelope.

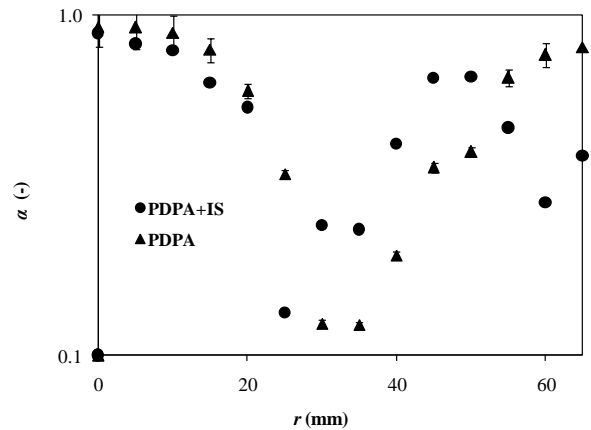


Fig 8. Void fraction ( $\alpha$ ) produced from a spray with changing radial position ( $r$ ) at 60D nozzle downstream. The mixing pressure was 482 kPa and air to liquid mass ratio was 2%.

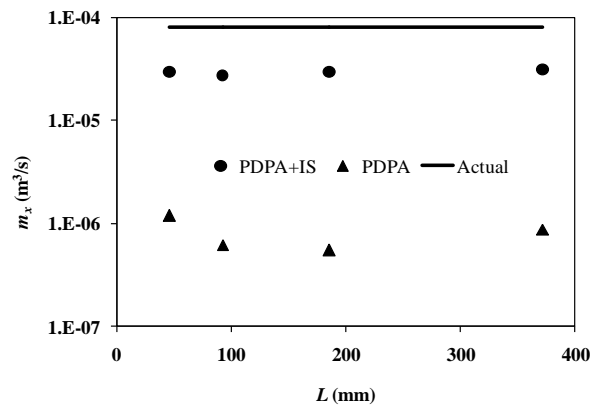


Fig 9. Integrated mass flux ( $m_x$ ) variation with axial distances from the tip of the nozzle. Here,  $D$  indicates diameter of the of the nozzle tip of 3.10 mm. The mixing pressure was 482 kPa and air to liquid mass ratio was 2%. Here, ' $L$ ' indicates the axial length of the spray.

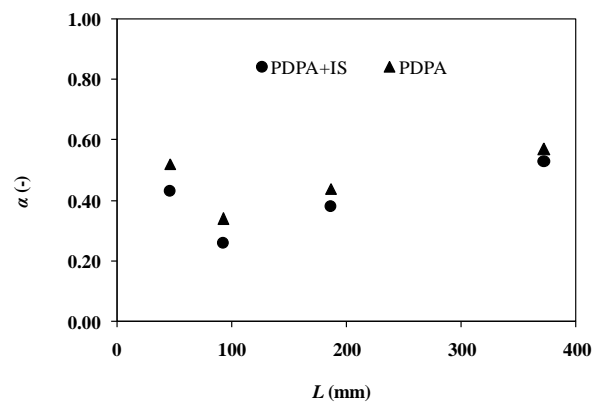


Fig 10. Integrated void fraction ( $\alpha$ ) profile with axial distances from the tip of the nozzle. The mixing pressure was 482 kPa and air to liquid ratio was 2%.

## 5. CONCLUSIONS

- Traditional laser diagnostics cannot reliably measure all droplet shapes in a multiphase dense spray.
- The PDPA method can reliably measure the droplet velocity in a dense spray.
- The IS method can reliably measure the droplet momentum in a dense spray.
- Combining the PDPA data with the IS data can estimate accurately the mass flux of a multiphase pulsating spray.

## 6. REFERENCES

[1] Ejim, C. E., M. A. Rahman, et al. (2010). "Effects of Liquid Viscosity and Surface Tension on Atomization in Two-Phase, Gas/Liquid Fluid Coker Nozzles." *FUEL* **89**: 1972-1882.

[2] Ejim, C. E., M. A. Rahman, et al. (2010). "Scaling Analysis of Nozzle Size on Atomization in Two-Phase, Gas-Liquid Nozzles." *Multiphase Science and Technology*: 22(2): 133-155..

[3] Rahman, M. A., T. Heidrick, et al. (2009). "A Critical Review of Two-Phase Gas/Liquid Industrial Spray Systems. International Review of Mechanical Engineering." *International Review of Mechanical Engineering* **3**(1): 110-125.

[4] Rahman, M. A., T. Heidrick, et al. (2009). "Characterizing the Two-Phase, Air/Liquid Spray Profile Using a Phase-Doppler-Particle-Analyzer." *IOP Journal of Physics – conference series* **147**: 1-15.

[5] Payri, R., S. Ruiz, et al. (2007). "On the Dependence of Spray Momentum Flux in Spray Penetration: Momentum Flux Packets Penetration Model." *Journal of Mechanical Science and Technology* **21**: 1100-1111

[6] Payri, R., J. M. Garcia, et al. (2005). "Using Spray Momentum Flux Measurements to Understand the Influence of Diesel Nozzle Geometry on Spray Characteristics." *Fuel* **84**: 551–561.

[7] Payri, R., B. Tormos, et al. (2008). "Spray Droplet Velocity Characterization for Convergent Nozzles with three Different Diameters." *Fuel* **87**: 3176–3182.

[8] Anantharamaiah, N., H. V. Tafreshi, et al. (2006). "A Study on Hydroentangling Waterjets and their Impact Forces." *Experiments in Fluids* **41**: 103–113.

[9] Bush, S., J. Bennett, et al. (1996). "Momentum Rate Probe for use with Two-Phase Flows." *Rev. Sci. Instrum.* **67**: 1878-85.

[10] Momber, A. W. (2001). "Energy Transfer during the Mixing of Air and Solid Particles into a High-Speed Waterjet: an Impact-Force Study." *Experimental Thermal*

and Fluid Science **25**: 31-41.

[11] Base, T. E., E. W. Chan, et al. (1999 ). "Nozzle for Atomizing Liquid in Two Phase Flow." US Patent 6003789.

[12] Phase Doppler particle analyser (PDPA)-Operations Manual, 1999, St Paul, MN: TSI.

[13] Albrecht, H. E., M. Borys, et al. (2003). *Laser Doppler and Phase Doppler Measurement Techniques*. Germany, Springer.

[14] Damaschke, N., G. Gouesbet, et al. (1998). "Response of Phase Doppler Anemometer Systems to Nonspherical Droplets." *Applied Optics* **37**(10): 1752-1761.

[15] Dodge, L. G., D. J. Rhodes, et al. (1987). "Drop-size Measurement Techniques for Sprays: Comparison of Malvern Laser-Diffraction and Aerometrics Phase/Doppler." *Applied Optics* **26**(11): 2144-2154.

[16] Gréhan, G., G. Gouesbet, et al. (1993). "Particle Trajectory effects in Phase Doppler Systems." *Part. Part. Syst. Charact.* **10**: 332-338.

[17] Gréhan, G., G. Gouesbet, et al. (1994). "Trajectory Ambiguities in Phase Doppler Systems: study of a near forward and a near backward geometry." *Part. Syst. Charact.* **11**: 133-144.

## 7. NOMENCLATURE

Symbol	Meaning	Unit
$D$	nozzle diameter	(m)
$P_u$	upstream pressure	(Pa)
$u_u$	upstream velocity	(m/s)
$P_s$	stagnation pressure	(Pa)
$u_s$	stagnation velocity	(m/s)
$\rho$	density of the fluid	(kg/m <sup>3</sup> )
$x$	axial location	(m)
$m_x$	mass flux in the axial direction	(kg/s.m <sup>2</sup> ) or (m <sup>3</sup> /s.m <sup>2</sup> )
$r$	radial distances	(m)
$F$	force	(N)
$L$	axial length of the spray	(m)
$\alpha$	void fraction	(-)
$\beta$	air to liquid mass ratio	(%)
$\rho$	density of the fluid	(kg/m <sup>3</sup> )
IS	Impulse sensor	
PDPA	Phase Doppler Particle Anemometer	
$N$	total number of droplets	
$T$	total condition	
$i$	local condition	

## **8. MAILING ADDRESS**

**Dr. Mohammad Aziz Rahman**

Postdoctoral Fellow

Department of Chemical and Materials Engineering,  
University of Alberta

7th Floor, Electrical & Computer

Engineering Research Facility (ECERF)

9107 - 116 Street, Edmonton, Alberta, Canada, T6G 2V4

Phone: 780-802-0728

**E-mail:** marahman@ualberta.ca